Available online at www.sciencedirect.com
ScienceDirect
Virology 374 (2008) 217–227
VIROLOGY
www.elsevier.com/locate/yviro

Heat shock 70 protein interaction with *Turnip mosaic virus* RNA-dependent RNA polymerase within virus-induced membrane vesicles

Philippe J. Dufresne [a], Karine Thivierge [a], Sophie Cotton [a], Chantal Beauchemin [b], Christine Ide [a], Eliane Ubalijoro [a], Jean-François Laliberté [b,*], Marc G. Fortin [a]

[a] *Department of Plant Science, McGill University, 21,111 Lakeshore, Ste-Anne-de-Bellevue, Quebec, Canada H9X 3V9*
[b] *Institut national de la recherche scientifique, Institut Armand-Frappier, 531 Boulevard des Prairies, Laval, Quebec, Canada H7V 1B7*

Received 9 November 2007; returned to author for revision 4 December 2007; accepted 9 December 2007
Available online 28 January 2008

Abstract

Tandem affinity purification was used in *Arabidopsis thaliana* to identify cellular interactors of *Turnip mosaic virus* (TuMV) RNA-dependent RNA polymerase (RdRp). The heat shock cognate 70-3 (Hsc70-3) and poly(A)-binding (PABP) host proteins were recovered and shown to interact with the RdRp *in vitro*. As previously shown for PABP, Hsc70-3 was redistributed to nuclear and membranous fractions in infected plants and both RdRp interactors were co-immunoprecipitated from a membrane-enriched extract using RdRp-specific antibodies. Fluorescently tagged RdRp and Hsc70-3 localized to the cytoplasm and the nucleus when expressed alone or in combination in *Nicotiana benthamiana*. However, they were redistributed to large perinuclear ER-derived vesicles when co-expressed with the membrane binding 6K-VPg-Pro protein of TuMV. The association of Hsc70-3 with the RdRp could possibly take place in membrane-derived replication complexes. Thus, Hsc70-3 and PABP2 are potentially integral components of the replicase complex and could have important roles to play in the regulation of potyviral RdRp functions.

Keywords: *Arabidopsis thaliana*; Heat shock protein; Hsp70; Poly(A)-binding protein; PABP; Potyvirus; RNA-dependent RNA polymerase; 6K-VPg-Pro; *Turnip mosaic virus*

Introduction

The RNA-dependent RNA polymerase (RdRp) is the core polypeptide that catalyzes the synthesis of RNA chains from both negative- and positive-strand templates of RNA viruses. The recruitment of the RdRp to membranes and its interaction with viral and host factors are critical for the efficiency, specificity and regulation of viral replication (Buck, 1996). Recent data from genome-wide screens in yeast (Jiang et al., 2006; Kushner et al., 2003; Panavas et al., 2005) have revealed the importance and multiplicity of viral–cellular interactions required for productive infection by positive-strand RNA viruses. A number of cellular proteins have been proposed as necessary for viral RdRp functions. Such factors were characterized following the co-purification of host proteins from the viral membrane replication complex and/or through the identification of host proteins that can directly interact with viral RdRps. The identification of host factors recruited to the replicase complex is of considerable interest as it sheds light on virus–cell interactions that facilitate infection and reveals the mechanistic components required for RNA replication.

In plants, different subunits of the translation initiation factor eIF3 were shown to interact with the membrane bound replicases of *Brome mosaic virus* (Quadt et al., 1993) and *Tobacco mosaic virus* (Osman and Buck, 1997), and the addition or immunodepletion of the eIF3 components modulated the *in vitro* RdRp activity of both viruses (Osman and Buck, 1997; Quadt et al., 1993). Similarly, the heat shock 70 protein (Hsp70) and the eukaryotic translation elongation factor 1A (eEF1A) were found in solubilized tobamovirus RdRp preparations (Nishikiori et al., 2006; Yamaji et al., 2006). In yeast, the Hsp70 homologues Ssa1/2p were recently reported to interact specifically with the

* Corresponding author. Fax: +1 450 686 5501.
E-mail address: jean-francois.laliberte@iaf.inrs.ca (J.-F. Laliberté).

0042-6822/$ - see front matter © 2007 Elsevier Inc. All rights reserved.
doi:10.1016/j.virol.2007.12.014

Cucumber necrosis virus (CNV) p33 replicase protein (Serva and Nagy, 2006). The activity of the replicase and level of viral replication correlated with the level of expression Ssa1/2p chaperones and it was suggested that Ssa1/2p is important for CNV replicase assembly.

Turnip mosaic virus (TuMV) is a *potyvirus* (Fauquet et al., 2005). Its positive single stranded RNA genome of almost 10 kilobases contains one long open reading frame and bears a viral genome-linked protein (VPg) covalently linked at its 5′ terminus and a poly(A) tail at the 3′ terminus (Nicolas and Laliberté, 1992). All TuMV-encoded proteins arise by synthesis of a large polyprotein followed by processing by viral proteinases. The C-terminal portion of this polyprotein yields two non-structural proteins that play important roles in replication: the 6K-VPg-Pro precursor polyprotein and the RdRp (Hong and Hunt, 1996).

A subset of the RdRp protein localizes to endoplasmic reticulum (ER) membranes where RNA synthesis takes place (Martin et al., 1995; Martin and Garcia, 1991; Schaad et al., 1997). The ER association of RdRp is likely due to its interaction with the 6K-VPg-Pro polypeptide (Léonard et al., 2004; Li et al., 1997; Restrepo-Hartwig and Carrington, 1994; Schaad et al., 1997). The 6K domain of the 6K-VPg-Pro polyprotein has been shown to be necessary for ER membrane targeting of VPg-Pro. For some potyviruses, the RdRp was also shown to accumulate in the nucleus (Baunoch et al., 1991; Restrepo et al., 1990; Riedel et al., 1998), where its function is unclear.

Potyviral RdRp interacts specifically with VPg-Pro (Daros et al., 1999; Fellers et al., 1998; Guo et al., 2001; Hong et al., 1995; Li et al., 1997). This interaction is thought to be essential since mutations that abolish or reduce the interaction have deleterious effects on replication (Daros et al., 1999; Li et al., 1997). One cellular interactor of the RdRp polymerase has been identified thus far for potyviruses. A yeast two-hybrid study has revealed the interaction of *Zucchini yellow mosaic virus* RdRp with the poly (A)-binding protein (PABP) of cucumber (Wang et al., 2000), but its biological significance has not been explored *in planta*.

In this study, we investigated host interactors of TuMV RdRp and found that *Arabidopsis thaliana* Hsc70-3 and PABP2 co-purify and directly interact with the viral RdRp. Upon inoculation, Hsc70-3 was relocalized to membranes and was co-immunoprecipitated with the RdRp polymerase from the microsomal fraction of an infected extract. Expression of 6K-VPg-Pro was sufficient to redirect the RdRp polymerase and host Hsc70-3 to large perinuclear ER-derived vesicles where replication likely takes place. Thus, Hsc70-3 and PABP2 are potentially integral components of the replicase complex and could have important roles to play in the regulation of potyviral RdRp functions.

Results and discussion

Identification of A. thaliana Hsc70-3 and PABP2 as TuMV RdRp interactors

To investigate cellular interactors of TuMV RdRp, we engineered an N-terminal fusion of the RdRp coding sequence with an improved tandem affinity purification (NTAPi) tag (Rohila et al., 2004). The NTAPi tag strategy has been used for the two-step isolation of highly purified native protein complexes in yeast and plants (Rigaut et al., 1999; Rohila et al., 2004; Rubio et al., 2005). The NTAPi tag is composed of the calmodulin binding peptide (CBP) domain, an AcTEV protease cleavage site (✂) and the *Staphylococcus aureus* Protein A (ProtA) domain preceded by the catalase intron (*CAT1*; Fig. 1A). The *Cauliflower mosaic virus* 35S promoter driven pNTAPi-RdRp construct was introduced in *Agrobacterium tumefaciens* and used for transformation of *A. thaliana* plants. Plants were also transformed with an NTAPi-tagged green fluorescent protein construct (pNTAPi-GFP; Rohila et al., 2004) to be used as a control for non-specific protein interactions.

A minimum of twenty putative *A. thaliana* transgenics for NTAPi-RdRp and NTAPi-GFP were evaluated by immunoblot analysis using anti-RdRp, anti-GFP, and/or anti-Protein A antibodies. The RdRp- and GFP-NTAPi fusions were detected in the crude cell lysate at the expected molecular masses of 82 kDa and 49 kDa, respectively (data not shown). Anti-CBP antibodies also allowed detection of RdRp- and GFP-NTAPi fusions at expected molecular masses of ~65 and 32 kDa respectively following human IgG sepharose beads chromatography and protease cleavage (see below, Fig. 1D).

NTAPi-RdRp lines were immune to TuMV infection as opposed to NTAPi-GFP lines, which showed typical TuMV symptoms and for which the viral capsid protein could be detected (data not shown). This is not unexpected as RdRp transgenics have previously been reported to be resistant to potyvirus infection (Audy et al., 1994; Jones et al., 1998; Simon-Mateo et al., 2003). RdRp levels were greatly reduced in TuMV-infected NTAPi-RdRp transgenics, which suggests that resistance could result from targeted RNA silencing of the RdRp sequence (data not shown).

Since NTAPi purification with TuMV-infected plant material was not possible, healthy 3-week-old *A. thaliana* NTAPi-RdRp plants were used. Protein extracts were incubated with IgG-coated beads and absorbed proteins then released by protease cleavage of the Protein A moiety. A second affinity purification step was performed by incubating the digested eluates with calmodulin-coated resin in presence of calcium and elution of native protein complexes was performed using an EGTA containing buffer. Eluates were subjected to SDS–PAGE and silver stained (Fig. 1B).

Mass spectrometric analysis was performed on two bands excised from a SDS–PAGE gel at 65 and 70 kDa, respectively. These bands were present in the RdRp purified extract but absent from GFP extract (Fig. 1B). Analysis of the 65 and 70 kDa bands in the RdRp purified extract allowed the identification of the RdRp and of another protein. Four peptide matches were obtained for the AtHsc70-3 protein in the 70 kDa band (Fig. 1C). Immunoblotting using a mouse monoclonal serum directed against human Hsc70/Hsp70 protein confirmed the co-purification of the host protein with the viral protein in the NTAPi-RdRp but not in the NTAPi-GFP extract (Fig. 1D). As Hsc70-3 is part of a multigene family (see below), it is possible that the sera used could react with other related Hsc70 proteins. To indicate this possibility, the general term “Hsc70” rather than specific “Hsc70-3”

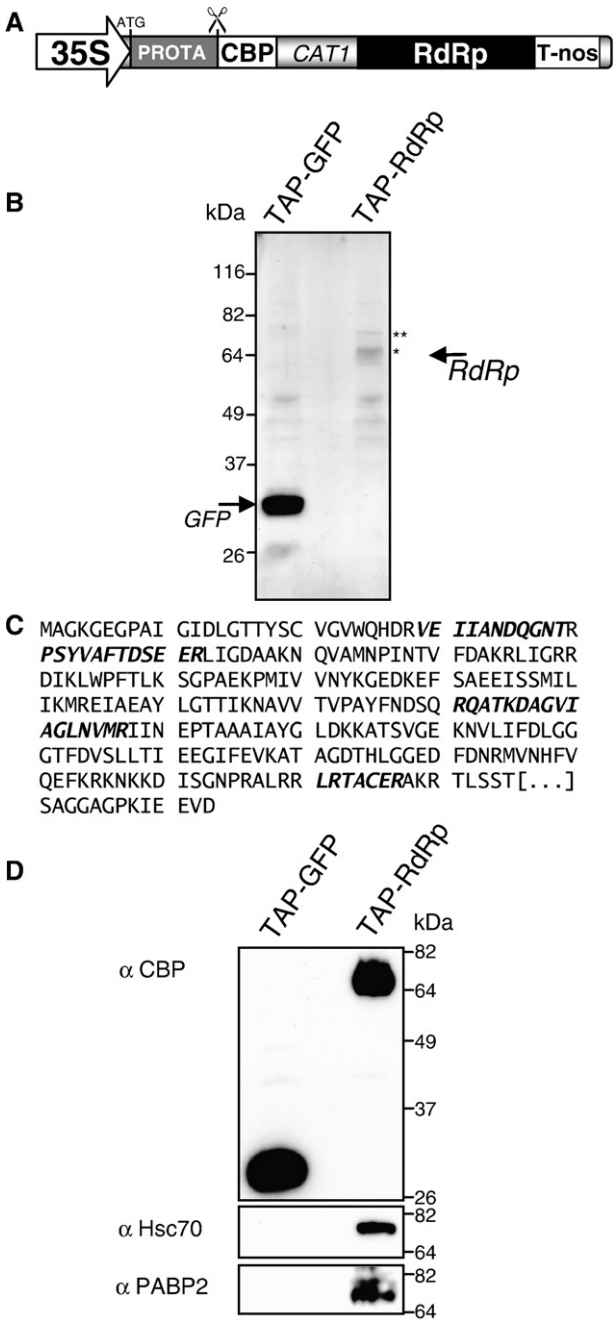

Fig. 1. Expression and purification of NTAPi-tagged RdRp fusion and identification of interactors in *A. thaliana*. (A) Diagram of NTAPi-RdRp construct used. Expression cassette is driven by 35S *Cauliflower mosaic virus* promoter (35S) followed by the coding sequence for *S. aureus* protein A (PROT A), AcTEV protease cleavage site (✂), calmodulin binding peptide (CBP), catalase intron 1 (*CAT1*), the RdRp, and ends with the nopaline synthase terminator (T-nos). (B) Silver stained SDS–PAGE of proteins co-purified in *A. thaliana* NTAPi-GFP (TAP-GFP) and NTAPi-RdRp (TAP-RdRp) lines following NTAPi purification. GFP and RdRp products are indicated with arrows. Positions of the excised bands used for mass spectrometric identification are indicated by asterisks. (C) Identification of *A. thaliana* Hsc70-3 as an RdRp interactor by mass spectrometric analysis (LC/MS). The four significant peptide matches are depicted in bold and italic. (D) Immunoblot analysis of cellular proteins purified in *A. thaliana* NTAPi-GFP (TAP-GFP) and NTAPi-RdRp (TAP-RdRp) lines. Proteins were separated by SDS–PAGE and analyzed by immunoblotting using rabbit antibodies directed against Hsc70, PABP2, or CBP moiety found in the NTAPi fusion.

denomination is used throughout the text when presenting immunoblots from complex plant protein extracts using these antibodies (Figs. 3–5). AtRNase L inhibitor 2 (At4g19210; NM11 8041) was also identified in the 70 kDa band but was not investigated further.

Based on previous work showing that the RdRp of *Zucchini yellow mosaic virus* interacted with PABP of *Cucumis sativus* in the yeast two-hybrid system (Wang et al., 2000), we also investigated and confirmed the presence of AtPABP2 in the NTAPi-RdRp extract but not in the NTAPi-GFP extract (Fig. 1D). The data presented here indicate that PABP/RdRp interaction is detected *in planta* in the *A. thaliana*/TuMV pathosystem and could be a broad conserved feature among other potyviruses.

PABP is an abundant RNA-binding protein which binds specifically to 3′ poly(A) tracts of mRNAs and is important factors in the regulation of protein synthesis initiation, mRNA maturation, and mRNA decay (Mangus et al., 2003). Interaction of PABP with the potyviral RdRp could be mechanistically analogous to that of PABP interacting with poliovirus 3CD polypeptide (polymerase precursor; $3D_{pol}$). The 3CD protein interacts with both PABP and poly(rC)-binding protein (PCBP). As PABP can still bind to poly (A) tail at 3′ end of viral genomic RNA and PCBP to the cloverleaf structure at its 5′ end, these interactions bridge the ends of the viral RNA and form a stable circular ribonucleoprotein complex thought to enhance replication/translation (Barton et al., 2001; Herold and Andino, 2001). Interaction of the RdRp with PABP could also position the RdRp on the polyadenylated 3′ end of the viral genomic RNA of TuMV to allow initiation of negative-strand synthesis.

Hsc70-3 and PABP2 interact with RdRp in vitro

Hsc70-3 and PABP2 co-purification with TuMV RdRp may be the result of direct interaction with the viral protein or occur through the intermediary of another protein that interacts with the RdRp. To test for the direct interaction of Hsc70-3 and PABP2 with the RdRp, an enzyme linked immunosorbent assay (ELISA)-based binding assay was performed. ELISA plate wells were coated with purified TuMV 6× histidine-tagged RdRp. The coated wells were then incubated with increasing concentrations of purified GST-tagged Hsc70-3 or PABP2. Complex retention was detected using an anti-GST antiserum. A saturation binding curve was observed for Hsc70-3 (Fig. 2A) and PABP2 (Fig. 2B). Binding was specific as no signal was detected in the absence of primary antibody (data not shown) or when GST-Hsc70-3 or GST-PABP2 was replaced with the GST protein. Overall this suggests that RdRp/Hsc70-3 and RdRp/PABP2 interactions are specific and result from direct protein–protein interaction.

In plant cells, Hsc70 is involved in protein folding, protein translocation, assembly of macromolecular complexes, and protein degradation functions (Craig et al., 1994; Mayer and Bukau, 2005). Hsc70-3 is a member of the Hsp70 chaperone family. In *A. thaliana*, this family comprises at least 14 members, five of which, including Hsc70-3, are predicted to be cytosolic (Lin et al., 2001; Sung et al., 2001). Hsc70-3 and three other cytosolic members were reported to be transcriptionally induced at high levels following TuMV infection (Aparicio et al.,

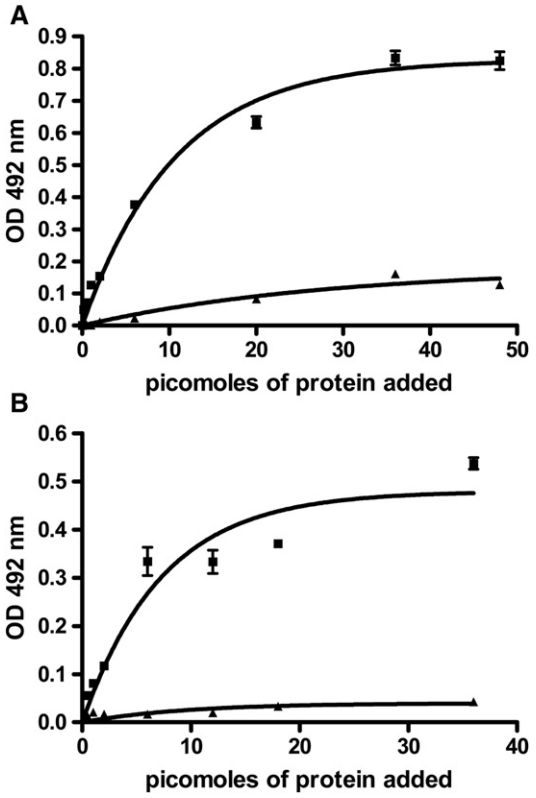

Fig. 2. *A. thaliana* Hsc70-3 and PABP2 interaction with RdRp *in vitro*. (A) Interaction of TuMV RdRp protein with *A. thaliana* Hsc70-3 protein in ELISA-based binding assays. Wells of a microtiter plate were coated with 25 pmol of *E. coli* purified 6×-histidine-tagged RdRp protein and incubated with increasing amounts of *E. coli* purified GST-tagged Hsc70-3 protein (■) or GST recombinant protein alone (▲). Retention of the complex was detected with polyclonal anti-GST antibodies. (B) Interaction of TuMV RdRp protein with *A. thaliana* PABP2 protein in ELISA-based binding assays. Wells of microtiter plate were coated with 25 pmol of *E. coli* purified 6×-histidine-tagged RdRp protein and incubated with increasing amounts of *E. coli* purified GST-tagged PABP2 protein (■) or GST recombinant protein alone (▲). Retention of the complex was detected with monoclonal anti-GST antibodies. In A and B, error bars are specified for GST control data, but the small S.E.M. values are masked by the data point symbols.

2005) and are expected to be abundant proteins in cells where viral replication takes place.

The identification of Hsc70 as a host factor interacting with TuMV RdRp is consistent with previous studies on the role of chaperones in viral replication and pathogenesis (Mayer, 2005; Sullivan and Pipas, 2001). Cellular chaperones have been found to co-purify with replicases and to be required for efficient replication of many classes of viruses (Brown et al., 2005; Glotzer et al., 2000; Hu et al., 2004; Kampmueller and Miller, 2005; Momose et al., 2002; Zylicz et al., 1989) including members of the bromo- (Tomita et al., 2003), tobamo- (Nishikiori et al., 2006), and tombus- (Serva and Nagy, 2006) virus genera. The interaction of Hsc70 with RdRp has been proposed to be necessary for the proper conformational arrangement of the replicase and its assembly at sites of viral replication (Serva and Nagy, 2006). Chaperone-assisted refolding has been shown to activate the polymerase activity and to confer template specificity. For example, *Brome mosaic virus* requires Ydj1, a yeast factor part of the heat shock protein family, for efficient negative strand RNA synthesis (Tomita et al., 2003). In the case of hepadnaviruses, Hsp40/70/90 binding is required for maintaining reverse transcriptase conformation and subsequent initiation of polymerase activity on the viral RNA template (Hu et al., 2002; Stahl et al., 2007). Furthermore, a recent report suggests that cellular dnaJ-like proteins in tobacco interact with *Potato virus Y* capsid protein and are required for efficient potyviral cell-to-cell movement (Hofius et al., 2007).

A subset of Hsc70 is redistributed to membrane and/or nucleus enriched fractions following TuMV infection

We have previously shown the redistribution of PABP2 to nuclear and membrane-associated fractions following TuMV infection (Beauchemin and Laliberté, 2007). In order to assess if the subcellular distribution of cytosolic Hsc70 could be modulated in a similar way in a TuMV infection context, nuclear and membrane fractionation experiments were conducted on mock and TuMV-infected *Brassica perviridis* plants.

Nuclei were purified from mock-inoculated and TuMV-infected leaves as described in Materials and methods. Ten micrograms of protein from the post-nuclear (S12) and purified nuclei (N) fractions were analyzed by immunoblot assay (Fig. 3A). In healthy plants, the bulk of Hsc70 was found in the post-nuclear fraction but was also detected, albeit weakly, in the nuclei fraction.

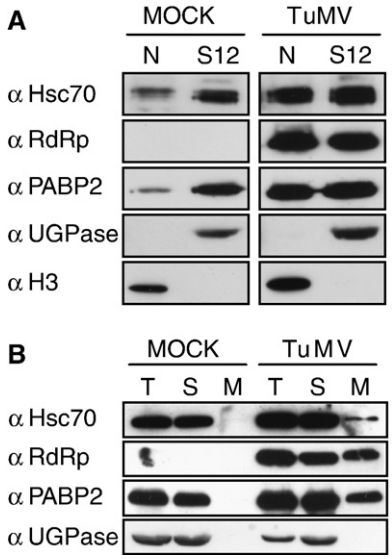

Fig. 3. Subcellular distribution of Hsc70, RdRp, and PABP2 in mock versus TuMV-infected *B. perviridis*. (A) Immunoblot analysis of nuclear and post-nuclear fraction proteins extracted from healthy (mock inoculated) or TuMV-infected plants. Leaves were homogenized and the extract centrifuged at 12,000×*g* through a sucrose cushion to separate the "soluble" fraction (S12) from crude nuclei (N). For each sample, 10 μg of protein was separated by SDS–PAGE. The experiment was repeated three times with different *B. perviridis* extracts and yielded similar results. (B) Immunoblot analysis of soluble and membrane-associated proteins from healthy (mock inoculated) or TuMV-infected *B. perviridis* plants. Total proteins (T) were extracted and soluble proteins (S) separated from membrane-associated proteins (M) by centrifugation at 30,000×*g*. Proteins were separated by SDS–PAGE and analyzed by immunoblotting using mouse/rabbit antibodies directed against Hsc70, RdRp, PABP2, UGPase, and/or histone H3.

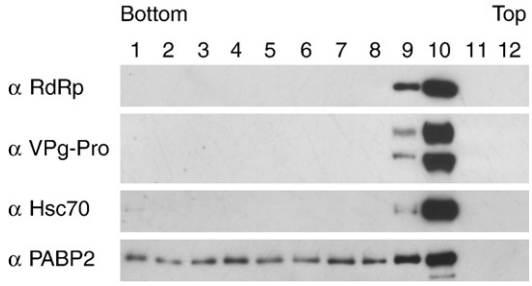

Fig. 4. Characterization of Hsc70 in microsomal fractions through a membrane flotation assay. P30 microsomal fractions were used. Fractions were collected from a step sucrose gradient and proteins in each fraction separated by SDS–PAGE and immunodetected with anti-RdRp, VPg-Pro, Hsc70, and PABP2 antibodies. Fraction 1 corresponds to the bottom and fraction 12 to the top of the gradient. For the anti-VPg-Pro immunoblot, the upper band corresponds to the membrane-associated 6K-VPg-Pro (55 kDa) and lower band to the VPg-Pro (49 kDa) polypeptide. PABP2 and 6K-VPg-Pro have previously been found associated with membrane fractions in flotation assays (Beauchemin and Laliberté, 2007) and are shown as positive controls.

However, when post-nuclear and nuclear fractions from infected plant material were analyzed, a different pattern emerged. Hsc70 was detected in equal amount in both nuclei and post-nuclear fractions (Fig. 3A). This redistribution to the nucleus parallels that observed for PABP in TuMV-infected plants. Relative abundance of Hsc70 was increased in both fractions when compared to mock control, which indicates that Hsc70 protein levels increased as a result of TuMV infection. This is supported by the observation that Hsc70-3-coding mRNA was transcriptionally induced at high levels following TuMV infection (Aparicio et al., 2005). Histone H3 and UDP-glucose pyrophosphorylase (UGPase), which are markers for the nucleus and cytoplasm, respectively, were detected in their respective fractions, indicating the absence of cytoplasmic contamination in the nuclear fraction and the absence of nuclear proteins in the post-nuclear fraction (Fig. 3A). The experiment was repeated three times with different *B. perviridis* extracts and yielded similar results.

Membrane fractionation was also performed on mock-inoculated and TuMV-infected *B. perviridis* leaves 12 days post-infection. Leaves were homogenized, and nuclei, chloroplasts, and cell wall debris were removed by centrifugation at 3700×*g*. Soluble proteins were then separated from membrane-associated proteins by centrifugation at 27,000×*g* and resuspended in same volume to allow quantitative evaluation. Total (T), soluble (S), and membrane-associated (M) proteins were separated by SDS–PAGE and subjected to immunoblot analysis with rabbit sera raised against recombinant forms of RdRp and AtPABP2, as well as serum raised against Hsc70. Hsc70 was absent from membrane-associated fraction and found strictly in the soluble fraction of healthy plants. However, in infected plants, Hsc70 was found in both soluble and membrane-enriched fractions (Fig. 3B). In our experiments, Hsc70 was consistently present in the membrane fraction in TuMV-infected extract and was not detected in the mock extract, this even after prolonged exposure. Again, this membrane association of Hsc70 parallels that of PABP. In both healthy and infected extracts, UGPase was detected only in the soluble and total protein extract fractions, which indicates the absence of cytoplasmic protein contamination in the membrane-enriched fractions.

The presence of Hsc70-3 in P30 fractions of TuMV-infected leaves may result from true membrane association or simply protein aggregation. To distinguish between these two possibilities, a membrane flotation assay was used (Beauchemin and Laliberté, 2007; Zhang et al., 2005). The membrane-enriched fraction (P30) was overlaid with a sucrose step gradient and subjected to centrifugation. Low density membranes and proteins associated with these membranes float to the upper part of the gradient while soluble proteins or aggregated proteins remain at the bottom. As shown in Fig. 4, the RdRp, 6K-VPg-Pro, and PABP2 rose towards the top of the gradient (fractions 9 and 10), indicating their association with membranes. Likewise, Hsc70 was found in fraction 9 and 10, confirming its membrane association.

Interaction of RdRp with Hsc70 and PABP within the membrane-associated fraction was tested by co-immunoprecipitation assay. P30 fraction from *A. thaliana* was solubilized with Triton X-100 and incubated with Protein G Sepharose beads coated with rabbit anti-RdRp, anti-AtPABP2, or pre-immune sera. Following centrifugation, proteins pelleted with the beads were eluted, separated by SDS–PAGE, and subjected to immunoblot analysis. Immunoprecipitation using the anti-TuMV RdRp serum allowed the recovery of Hsc70 and PABP2 (Fig. 5A). No protein was detected in the immunoblot with the pre-immune serum or with the Protein G Sepharose negative controls. No protein was

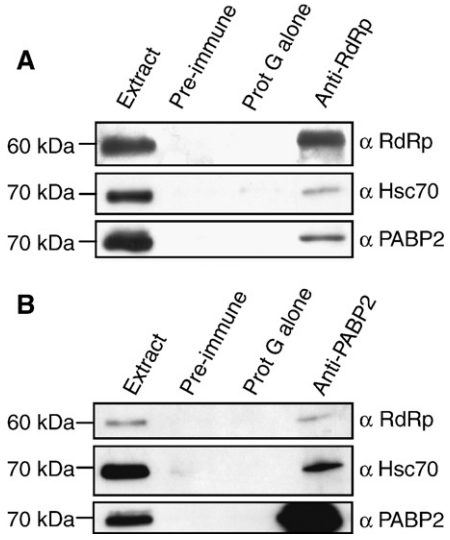

Fig. 5. The RdRp protein is complexed with *A. thaliana* Hsc70 and PABP2 proteins in membrane-enriched fraction of TuMV-infected plants. (A) Immunoprecipitation of Hsc70 and PABP2 with RdRp antibody in membrane-enriched fraction (30,000×*g* pellet) in TuMV-infected *A. thaliana* plants. (B) Immunoprecipitation of RdRp and Hsc70 with PABP2 antibody in membrane-enriched fraction (30,000×*g* pellet) in TuMV-infected *A. thaliana* plants. The immunoprecipitates, total extracts, pre-immune serum, and protein G sepharose controls were subjected to SDS–PAGE and immunoblotted with antibodies against TuMV RdRp, Hsc70, and PABP2. Lane "Extract" indicates the total 30,000×*g* membrane-associated protein extract. Lanes "anti-RdRp" and "anti-PABP2" indicate the immunoprecipitates immobilized onto Sepharose fast Flow protein G beads matrix with the RdRp or PAPB2 antibody. Pre-immune antibodies coupled to protein G sepharose ("pre-immune" lane) and protein G sepharose alone ("Prot G alone" lane) were used as negative controls.

immunoprecipitated when a healthy plant fraction was used (data not shown). Similarly, RdRp and Hsc70-3 were precipitated with the anti-PABP2 serum (Fig. 5B). These experiments indicate that RdRp/Hsc70/PABP2 complexes are formed in the membrane-associated fraction and it also raises the possibility of tripartite interactions between RdRp, PABP2, and Hsc70.

RdRp/Hsc70-3 complex localizes to cytoplasmic vesicles induced by 6K-VPg-Pro

To assess if the RdRp could be responsible for the membrane association of Hsc70-3, RdRp and AtHsc70-3 were fused to the fluorescent protein tags (GFP, mCherry, or DsRed2) and expressed transiently by agroinfiltration in *Nicotiana benthamiana*, a host of TuMV. Proper expression of the fluorescent fusions was assessed by immunoblot analyses using rabbit sera raised against RdRp, Hsc70, or GFP. In each case, a signal corresponding to the expected molecular mass of the analyzed protein was observed, indicating that full-length proteins had been expressed (data not shown).

To facilitate subcellular localization of cytoplasmic and membrane structures, GFP and DsRed2 markers with or without ER targeting signals were co-expressed along with the fluorescent fusion proteins (Beauchemin et al., 2007; Zhang et al., 2005). Fluorescence of GFP-RdRp and Hsc70-3-DsRed2 was observed in the nucleus (excluding nucleolus) and cytoplasm (Figs. 6B and D, respectively). Merging of the fluorescence with that of free DsRed2 or GFP (Figs. 6A and E, respectively) showed co-localization (Figs. 6C and F, respectively). No co-localization was observed when GFP-RdRp was expressed with DsRed2-ER or Hsc70-3 with GFP-ER markers (data not shown). When produced alone, RdRp and Hsc70-3 were thus soluble proteins. The cytoplasmic distribution of Hsc70-3 when fused to GFP is also in agreement with data from Prokhnevsky et al. (2005). Upon co-expression, the distribution of Hsc70-3-DsRed2 (Fig. 6G) and GFP-RdRp (Fig. 6H) remained nuclear and cytoplasmic (Fig. 6I). PABP and RdRp also remained soluble and co-localized mostly to the cytoplasm following co-expression (Figs. 6J to L). Thus, expression of RdRp is not sufficient for redistribution of Hsc70-3 or PABP2 to membranes, indicating that a third partner is likely required.

6K-VPg-Pro induces the formation of cytoplasmic vesicles that harbor the viral replication complex (Léonard et al., 2004; Li et al., 1997; Restrepo-Hartwig and Carrington, 1994; Schaad et al., 1997). Its interaction with the RdRp has been demonstrated for TEV and TVMV (Fellers et al., 1998; Li et al., 1997). We consequently investigated whether expression of 6K-VPg-Pro was responsible for membrane association of RdRp and Hsc70-3.

Upon co-expression of 6K-VPg-Pro-mCherry (Fig. 7A) with fluorescent construct GFP-RdRp (Fig. 7B), most of the merged fluorescence signal was found within cytoplasmic vesicular structures (Fig. 7C), similar to those observed when 6K-VPg-Pro-GFP is expressed alone (Beauchemin et al., 2007). These vesicles were most often perinuclear and typically exceeded in diameter those of 6K-VPg-Pro-GFP, with an average maximum diameter of 16.7 μm (S.E.M.±1.7; $n=8$). On the other hand, the

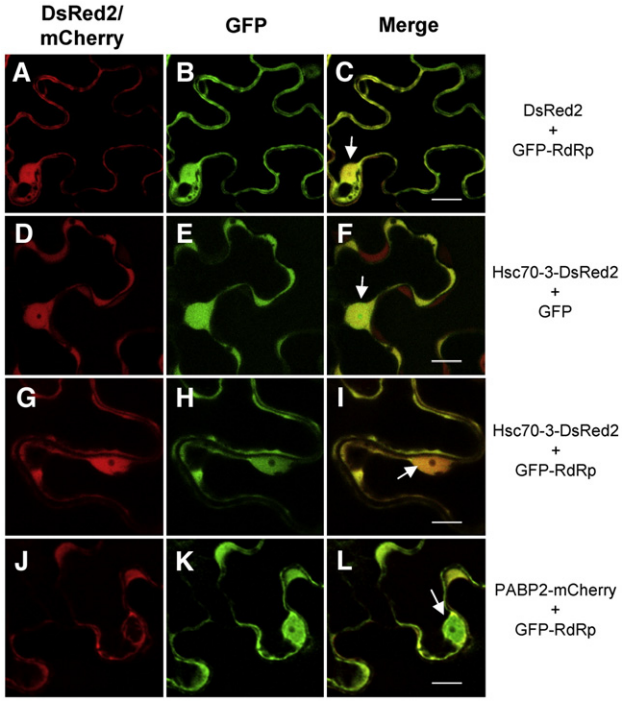

Fig. 6. RdRp/Hsc70-3 and RdRp/PABP2 co-localization *in planta*. Subcellular localization of RdRp, Hsc70-3, and PABP2. *N. benthamiana* leaves were infiltrated with *A. tumefaciens*, and expression of fluorescent proteins was visualized by confocal microscopy 2–4 days later. *A. tumefaciens* suspensions contained binary Ti plasmids encoding DsRed2 and GFP-RdRp (A to C), Hsc70-3-DsRed2 and GFP (D to F), Hsc70-3-DsRed2 and GFP-RdRp (G to I), and GFP-RdRp and PABP2-mCherry (J to L). Scale bar=15 μm. All agroinfiltrations were performed with the P19 inhibitor of silencing as previously described (Beauchemin et al., 2007). Nuclei are indicated with white arrows in the merged panel.

Hsc70-3-DsRed2 fluorescence did not specifically co-localize with the vesicles induced by 6K-VPg-Pro-GFP (Figs. 7D to F).

We then tested if membrane association of Hsc70-3 in infected cells was promoted by its interaction with the RdRp/6K-VPg-Pro complex. First, we looked if expression of 6K-VPg-Pro-ct (Beauchemin et al., 2007), a non-fluorescent form of the viral protein, could induce the formation of cytoplasmic vesicles, within which RdRp would be found. RdRp-GFP, DsRed2-ER, and 6K-VPg-Pro-ct were co-expressed in *N. benthamiana* leaves. DsRed2-ER showed the expected reticulate fluorescent pattern for an ER protein, with the added emergence of a large perinuclear vesicle (Fig. 7G), such vesicle being induced by 6K-VPg-Pro-ctGFP. Similarly to when it was co-expressed with 6K-VPg-Pro-mCherry, RdRp-GFP showed the same fluorescent pattern (compare Fig. 7B with H) and co-localized with the perinuclear vesicle (Fig. 7I). Similar vesicles were observed upon co-infiltration of both GFP-RdRp and Hsc70-3-DsRed2 constructs with 6K-VPg-Pro-ctGFP in *N. benthamiana* leaves. Most of the fluorescence emitted by Hsc70-3 DsRed2 (Fig. 7J) and GFP-RdRp (Fig. 7K) was found within 6K-VPg-Pro induced vesicles, where strong co-localization was observed (Fig. 7L). The size of these cytoplasmic vesicles was similar to those observed when GFP-RdRp and 6K-VPg-Pro-mCherry were co-expressed (14.9 μm: S.E.M.±1.1; $n=7$). Thus, the expression of both RdRp and 6K-VPg-Pro-

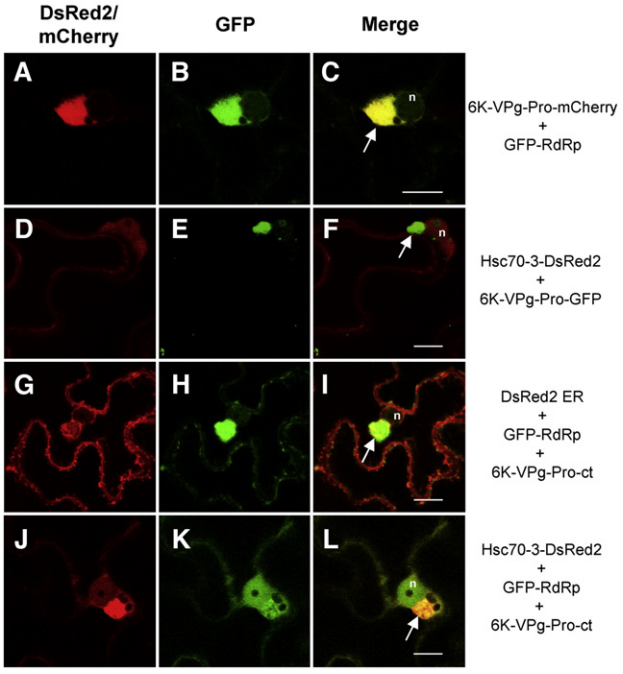

Fig. 7. RdRp and Hsc70-3 are redirected to membranous vesicles when co-expressed with 6K-VPg-Pro. Subcellular localizations of RdRp and Hsc70-3 when co-expressed with 6K-VPg-Pro. *N. benthamiana* leaves were infiltrated with *A. tumefaciens*, and expression of fluorescent proteins was visualized by confocal microscopy 2–4 days later. *A. tumefaciens* suspensions contained binary Ti plasmids encoding 6K-VPg-Pro-mCherry and GFP-RdRp (A to C), Hsc70-3-DsRed2 and 6K-VPg-Pro-GFP (D to F), DsRed2-ER, GFP-RdRp, and non-fluorescent 6K-VPg-Pro-ct (G to I), and Hsc70-3-DsRed2, GFP-RdRp, and non-fluorescent 6K-VPg-Pro-ct (J to L). Scale bar=15 μm. All agroinfiltrations were performed with the P19 inhibitor of silencing as previously described (Beauchemin et al., 2007). Nuclei are indicated with the letter "n" and "6K-VPg-Pro"-induced vesicles with white arrows in the merged panel.

GFP appears to be required to redirect Hsc70-3 to these vesicles. This suggests that Hsc70-3 needs to interact with the RdRp for efficient translocation to 6K-VPg-Pro vesicles.

The interaction of Hsc70-3 with the RdRp and its co-localization with the replicase on membranes suggest that it could be an integral part of the potyvirus replicase complex as seen for other family of plant positive RNA viruses (Nishikiori et al., 2006; Serva and Nagy, 2006; Tomita et al., 2003). Localization data emphasize the role of 6K-VPg-Pro as an important determinant of subcellular redistribution of viral and recruited host components. 6K-VPg-Pro polypeptide alone is sufficient to redirect the RdRp and Hsc70-3 to ER-derived vesicle. This is in addition to the host factors PABP and eIF(iso)4E (Beauchemin et al., 2007; Beauchemin and Laliberté, 2007), which have also been observed to be redistributed in vesicles budding from the ER when co-expressed with 6K-VPg-Pro or to nucleolus when expressed with VPg-Pro. The recruitment of necessary host and viral components to a membrane structure would likely protect the replication machinery from external nucleases and proteases, as seen for instance with for *Brome mosaic virus* (Schwartz et al., 2002) and hepatitis C virus (Aizaki et al., 2004; El-Hage and Luo, 2003) and have positive effects of viral replication/translation. Additionally, it would provide a stable framework for the polymerase and host/virus components to assemble into a functional replication complex.

Conclusion

Identification of host PABP and Hsc70-3 as RdRp-interacting proteins and their targeting to 6K-VPg-Pro putative replication vesicles emphasizes their potential role in replication of TuMV. Hsc70-3 and PABP2 are potentially integral components of the potyvirus replicase complex and assessment of both proteins capacity to regulate the RdRp activity should be pursued. We likely have overlooked many other cellular factors that are part of TuMV replicase complex with the purification strategy used here. Purification and identification of the proteins present within 6K-VPg-Pro-induced vesicles appear as one productive approach that could be employed to characterize the composition of TuMV replicase complex in the future.

Materials and methods

Plant and bacterial expression constructs

The pNTAPi-RdRp *Cauliflower mosaic virus* (CaMV) 35S promoter driven plant expression vector (Fig. 1A) was constructed as follow. RdRp was PCR-amplified from full-length TuMV UK1 cDNA clone p35Tunos (Sanchez et al., 1998) using primers RdRp-GWF and RdRp-GWR (Table S1). The purified PCR product was cloned in pENTR/D-TOPO vector (Invitrogen) and the attL sites within this clone were used to clone the RdRp in the pNTAPi vector (Rohila et al., 2004) with LR clonase (Invitrogen). The control pNTAPi-GFP vector (Fig. 1A) has been described previously (Rohila et al., 2004).

For construction of the vector coding for the N-terminus 6× histidine-T7 tag full-length RdRp fusion protein, TuMV RdRp sequences were PCR-amplified from p35Tunos using primers RdRp-*Bam*HI and RdRp-*Not*I (Table S1). The amplified fragments were digested with *Bam*HI/*Not*I and cloned into similarly digested pET28(a) (Novagen).

For construction of the vector coding for the N-terminus GST fusion of *A. thaliana* Hsc70-3 (At3g09440; GenBank accession no. NM111778) and PABP2 (At4g34110; GenBank accession no. L19418) proteins, sequences were PCR-amplified from validated SSP gold standard full-length ORF clones C104970 and U22035 (Yamada et al., 2003) using primers Hsc70-3F-*Eco*RI and Hsc70-3R-*Eco*RI, and PABP2-*Eco*RI and PABP2-*Not*I (Table S1). The amplified fragments were digested with *Bam*HI/*Not*I or *Eco*RI and cloned into similarly digested pGEX-6P1 (GE Healthcare).

Plasmids for co-localization experiments were constructed as follows. EGFP (Clontech) gene was excised with *Xba*I/*Eco*RI from pGreen/EGFP (Beauchemin et al., 2007) and inserted into similarly digested backbone of pCambia/DsRed2, resulting in plasmids pCambia/EGFP. The cDNA for Hsc70-3 and RdRp were amplified with the RdRpF EGFP-*Sma*I and RdRpR EGFP-*Sal*I primers, or Hsc70-3F DsRed2-*Xba*I and Hsc70-3R DsRed2-*Bam*HI (Table S1) and inserted into the *Sal*I/*Sma*I sites of pCambia/EGFP or *Bam*HI/*Xba*I sites of pGreen/DsRed2. The

resulting plasmids were identified as pGreen/Hsc70-3-DsRed2 and pCambia/GFP-RdRp. 6K-VPg-Pro sequence gene was excised with *Hin*dIII/*Bam*HI from pGreen/6K-VPg-Pro-GFP plasmid and inserted into similarly digested backbone of pCambia/PABP-mCherry, resulting in plasmids pCambia/6K-VPg-Pro-mCherry. The plasmids pGreen/GFP, pCambia/PABP-mCherry, pCambia/DsRed2, pGreen/6K-VPg-Pro-GFP, and pGreen/6K-VPg-Pro-ct have previously been described (Beauchemin et al., 2007; Beauchemin and Laliberté, 2007). All PCR amplifications were performed with *Pfu* Turbo polymerase (Stratagene) and all plasmid constructs verified by sequencing.

Plant material and growth conditions: generation of RdRp-NTAPi transgenic A. thaliana

A. thaliana plants used in this study are all of the Columbia-0 ecotype. Col-0 plants were transformed with the pNTAPi-RdRp or pNTAPi-GFP constructs using a modified version of the floral dipping technique (Martinez-Trujillo et al., 2004). T_1 transformants were sown on a peat based mix and selected with glufosinate-ammonium herbicide (0.00578%). *A. thaliana* NTAPi-RdRp and NTAPi-GFP T_1 lines were evaluated by immunoblot detection of NTAPi-tagged RdRp or GFP in pools of T_2 lines by using anti-RdRp, anti-GFP, and/or anti-Protein A antibodies. Lines were further selected by screening T_2 progenies for glufosinate-ammonium resistance. Only the lines with resistance/sensitivity ratio of approximately 3:1, indicative of a single T-DNA insertion event, were chosen and used in our experiments. All lines used for NTAPi purification were thus homozygous lines at T_3 or T_4 generation with stable expression.

NTAPi purification procedure

Three-week-old NTAPi–RdRp and NTAPi-GFP plants (7.5 g, fresh weight) were ground in liquid nitrogen, thawed in 2 volumes of extraction buffer (50 mM Tris–HCl, pH 7.6, 150 mM NaCl, 10% glycerol, 1 mM DTT, 0.1% IGEPAL, and 1× Complete protease inhibitor; Roche) and centrifuged twice at 30,000×*g* for 20 min. Supernatants were incubated with 400 µl of human IgG sepharose beads (Amersham Bioscience) for 1.5 h at 4 °C with gentle rotation. Beads were washed 3 times with 10 ml of extraction buffer and once with 10 ml of cleavage buffer (50 mM Tris–HCl, pH 7.6, 150 mM NaCl, 10% glycerol, 0.5 mM EDTA, 0.1% IGEPAL, 1 mM DTT, 1 µM E-64 protease). Elution from IgG beads was performed by incubation with 20 µl (200 units) of AcTEV protease (Invitrogen) in 3 ml of cleavage buffer at 10 °C for 2 h with gentle rotation. Column was drained and washed with 1 ml of cleavage buffer. Six milliliters of calmodulin binding buffer (50 mM Tris–HCl, pH 7.6, 150 mM NaCl, 10 mM β-mercaptoethanol, 1 mM magnesium acetate, 1 mM imidazole, 2 mM $CaCl_2$, 0.1% IGEPAL) and 12 µl of 1M $CaCl_2$ was added to the pooled eluates and loaded onto 400 µl of calmodulin affinity resin (Stratagene) and incubated for 1.5 h at 4 °C with gentle rotation. After washing the column three times with 10 ml of calmodulin binding buffer, elution was performed with CBP elution buffer (50 mM Tris–HCl, pH 8.0, 150 mM NaCl, 0.1% IGEPAL, 5 mM EGTA, 10 mM β-mercaptoethanol, and 1 mM imidazole).

Proteins were concentrated using StrataClean Resin (Stratagene) and separated on an SDS–PAGE gel. Protein bands were visualized by immunoblotting using the rabbit anti-calmodulin binding protein epitope tag (Upstate cell signaling solutions) or ProtA mouse monoclonal antibodies (Sigma-Aldrich), silver staining (Silver staining Plus; Bio-Rad) or Bio-Safe Coomassie blue staining (Bio-Rad). The NTAPi purification procedures were repeated independently four times and yielded similar results.

Mass spectrometry analysis

Coomassie or silver stained bands from 1D acrylamide gel were excised and digested with trypsin on a MassPrep robotic workstation (PerkinElmer). Digested peptides were run for an hour on an LC-QToF (Micromass), a tandem MS–MS at Genome Quebec Center at McGill University. Peak identification was carried using Mascot software (Matrix Science).

Mouse monoclonal and rabbit polyclonal antibodies

The primary antibodies were used as follows: anti-PABP2 1:2000; anti-TuMV RdRp 1:1000; mouse monoclonal Anti-Hsp70/Hsc70 1:1000 (Stressgen); rabbit polyclonal anti-Hsp70/Hsc70 (Stressgen) 1:1000; mouse rabbit polyclonal anti-CBP domain (Upstate Biotech) 1:1000; rabbit polyclonal Anti-UGPase (Agrisera) 1:1000; rabbit polyclonal Anti-GFP (Molecular Probes) 1:1000; and goat polyclonal anti-Histone H3 (H3; Santa Cruz Biotechnology) 1:250.

The recombinant clone pET-RdRp in *E. coli* BL21(DE3) cells was used for antibody production as follows. Full-length coding sequence of RdRp polymerase of Qc strain (Nicolas and Laliberté, 1992) was cloned in frame in the pET11d vector (Novagen). The resulting recombinant protein was overproduced in *E. coli* and purified as insoluble inclusion bodies. Inclusion bodies were resuspended in TBS buffer and used for rabbit injection and serum production at McGill University Animal Resources Center.

SDS–PAGE and immunoblotting

Proteins were separated in 8 to 11% SDS gel (Laemmli, 1970), transferred onto nitrocellulose (Bio-Rad) by wet electroblotting, and were reacted with the appropriate antibodies. The antigen–antibody complexes were visualized using a horseradish peroxidase coupled goat anti-rabbit IgG under standard conditions. Complexes were visualized with Super Signal West Pico substrate (Pierce).

Expression and purification recombinant proteins in E. coli

For purification of GST-tagged Hsc70-3, PABP2, or the GST tag itself, a 20 ml overnight culture of *E. coli* BL21 cells containing the recombinant plasmid pGEX6P1-Hsc70-3, pGEX6P1-PABP2, or pGEX6P1 vector alone was used to inoculate 500 ml of LB media containing 75 µg/ml of carbenicillin. Cells were grown at 32 °C to an OD_{600} of 0.6. Protein expression was induced with 0.4 mM of IPTG for 4.5 h for GST-Hsc70-3 and for

2 h at 30 °C for PABP2-GST and GST. Bacterial cells were resuspended in 20 ml of phosphate buffered saline solution (PBS; 4.3 mM Na_2HPO_4, 1.47 mM KH_2PO_4, 137 mM NaCl, 2.7 mM KCl, pH 7.3) supplemented with 1 mM DTT, 40 mg of lysozyme, and 1× complete EDTA-free protease inhibitor. The cells were disrupted by sonication and supplemented with 1% Triton-X-100. Lysate was centrifuged at 30,000×*g* for 30 min at 4 °C. The supernatant was filtered through a 0.45 μm Millex HV PVDF filter (Millipore) and used for affinity purification of either GST-PABP2, GST-Hsc70-3, or GST on glutathione sepharose 4B (GE Healthcare) according to manufacturer's protocol.

For purification of histidine-tagged RdRp of TuMV, a 5 ml overnight culture of *E. coli* BL21(DE3) cells containing the recombinant plasmid pET28(a)-RdRp was used to inoculate 500 ml of LB media containing 50 μg/ml of kanamycin. Cells were grown at 32 °C to an OD_{600} of 0.4 to 0.6. Protein expression was induced with 1 mM of IPTG for 1.5 h at 30 °C. Bacterial cells were resuspended in 5 ml of buffer A (50 mM sodium phosphate buffer pH 8.0, 300 mM NaCl, 5 mM β-mercaptoethanol, 0.1% Tween-20, 10% glycerol, 1× complete EDTA-free protease inhibitor). The cells were disrupted by sonication and the resulting lysate centrifuged at 30,000×*g* for 30 min at 4 °C. The supernatant was used for immobilized metal affinity purification on Talon resin (BD Biosciences). Resin was washed with buffer A supplemented with 10 mM imidazole and proteins eluted with buffer B (20 mM Tris–HCl pH 7.5, 300 mM NaCl, 250 mM imidazole, 2.5 mM DTT).

Concentration of all recombinant proteins produced was measured using a Bradford assay (Bio-Rad) using bovine serum albumin as standard. Protein purity and molecular weight were assessed by Coomassie staining and immunoblot analysis using monoclonal anti-histidine, monoclonal anti-GST, polyclonal anti-RdRp, and/or anti-Hsc70 (data not shown).

RdRp/Hsc70 and RdRp/PABP ELISA-based binding assays

RdRp protein (100 μl of protein at 15 ng μl^{-1} in PBS buffer) was adsorbed to wells of a polystyrene plate (Costar) by incubation at 4 °C for 2 h and wells were blocked with 5% milk PBS solution for 2 h at room temperature. GST-Hsc70-3 or GST-PABP2 proteins were diluted in PBS with 1% milk and 0.1% Tween-20 and incubated for 2 h at 4 °C in the previously coated wells. Detection of retained protein was achieved with a mouse monoclonal (Novagen) or polyclonal (Molecular Probes) anti-GST-tag antibody and horseradish peroxidase-coupled goat anti-mouse or anti-rabbit immunoglobulin (Pierce). Between each incubation, wells were washed four times with PBS supplemented with 0.05% Tween-20. Enzymatic reactions were performed in 100 μl of OPD citrate buffer (50 mM citric acid, 100 mM sodium phosphate dibasic, pH 5.0, 0.5 mg/ml *o*-phenylenediamine dihydrochloride, and 0.1% H_2O_2) and stopped with a solution of 3 M H_2SO_4. Absorbance was measured at 492 nm. The S.E.M. was calculated for three biological replicates from a minimum of two technical replicates.

Subcellular fractionation and membrane flotation assay

Membrane fractionation and membrane flotation assays were performed as previously described on mock inoculated and/or TuMV-infected *B. perviridis* leaves (Beauchemin et al., 2007; Beauchemin and Laliberté, 2007). Nuclear fractionation was performed on the same plant material using CelLytic Plant nuclei isolation/extraction kit (Sigma) according to manufacturer's protocol, and nuclei recovered by pelleting at 12,000×*g* through a 3.2 M sucrose cushion resulting in a soluble fraction (S12) and nuclear pellet (N). Ten micrograms was diluted in 1:5 in SDS loading buffer and subjected to SDS–PAGE and immunoblotting.

In vivo co-immunoprecipitation analyses

For co-immunoprecipitation analyses, 1 g of TuMV-infected or healthy *A. thaliana* tissue was homogenized on ice in 7.5 ml of IP buffer (50 mM Tris–HCl pH 7.5, 50 mM KCl, 200 mM NaCl, 5 mM EDTA, 5% glycerol, and 1× Complete EDTA-free protease inhibitor). Extract was centrifuged twice at 4000×*g* to remove cellular debris and at 30,000×*g* for 20 min. The 30,000×*g* pellet was washed and resuspended in 4 ml of IP buffer supplemented with 1% Triton X-100. After centrifugation, the supernatants were passed through a 0.45 μm MillexHV PVDF filter. For the pull-down assay, 2 ml of the clarified extract was incubated with 40 μl of protein G sepharose 4 Fast flow beads (Amersham Bioscience) previously coupled to 7.5 μl rabbit anti-RdRp, anti-AtPABP2, or pre-immune sera. The matrix beads were washed five times with 1.25 ml of IP buffer. The immunoprecipitated proteins were subsequently released by boiling in 2× SDS Laemmli sample buffer. The protein blot of the immunoprecipitate was performed as described above except that an HRP-coupled monoclonal anti-rabbit IgG specific to Light Chain (Jackson ImmunoResearch) was used to reduce non-specific background.

Agroinfiltration and confocal microscopy

Vectors containing genes for fluorescent and fusion proteins were introduced into *A. tumefaciens* AGL1 by electroporation. Agroinfiltration in *N. benthamiana* and confocal microscope visualization was carried as previously described (Beauchemin et al., 2007). Fluorescence was visualized between 2 and 4 days post-infiltration by confocal microscopy. No notable differences in cellular localization of the fluorescent proteins expressed were observed during this time period with the constructs used. Fluorescence was generally observed in 40% to 60% of the cells in the infiltrated area. Images were collected with a charge-coupled-device camera and treated with Image J (http://rsb.info.nih.gov/ij/) software.

Acknowledgments

We thank Dr. Fernando Ponz for the TuMV clone and Dr. Michael Fromm (University of Nebraska, Lincoln, USA) for pNTAPi and pNTAPi-GFP vectors. We wish to thank Olivier LeGall, Sylvie German, Thierry Michon, and Valérie Nicaise (IBVM, INRA, Bordeaux, France) for helpful discussions and Hélène Sanfaçon (Pacific Agri-Food Research Centre, Summerland, Canada) for critical reading of the manuscript. This work was supported by grants to MGF and JFL from the National

Science and Engineering Research Council of Canada and from the Québec Fonds de la recherche sur la nature et les technologies fund in the form of scholarships.

Appendix A. Supplementary data

Supplementary data associated with this article can be found, in the online version, at doi:10.1016/j.virol.2007.12.014.

References

Aizaki, H., Lee, K.-J., Sung, V.M.H., Ishiko, H., Lai, M.M.C., 2004. Characterization of the hepatitis C virus RNA replication complex associated with lipid rafts. Virology 324, 450–461.

Aparicio, F., Thomas, C.L., Lederer, C., Niu, Y., Wang, D., Maule, A.J., 2005. Virus induction of heat shock protein 70 reflects a general response to protein accumulation in the plant cytosol. Plant Physiol. 138, 529–536.

Audy, P., Palukaitis, P., Slack, S.A., Zaitlin, M., 1994. Replicase-mediated resistance to potato virus Y in transgenic tobacco plants. Mol. Plant-Microb. Interact. 7, 15–22.

Barton, D., O'Donnell, B., Flanegan, J., 2001. 5′ cloverleaf in poliovirus RNA is a *cis*-acting replication element required for negative-strand synthesis. EMBO J. 15, 1439–1448.

Baunoch, D.A., Das, P., Browning, M.E., Hari, V., 1991. A temporal study of the expression of the capsid, cytoplasmic inclusion and nuclear inclusion proteins of *Tobacco etch potyvirus* in infected plants. J. Gen. Virol. 72, 487–492.

Beauchemin, C., Boutet, N., Laliberté, J.-F., 2007. Visualization of the interaction between the precursors of VPg, the viral protein linked to the genome of *Turnip mosaic virus*, and the translation eukaryotic initiation factor iso 4E *in planta*. J. Virol. 81, 775–782.

Beauchemin, C., Laliberté, J.-F., 2007. The poly(A) binding protein is internalized in virus-induced vesicles or redistributed to the nucleolus during *Turnip mosaic virus* infection. J. Virol. 81, 10905–10913.

Brown, G., Rixon, H.W.M., Steel, J., McDonald, T.P., Pitt, A.R., Graham, S., Sugrue, R.J., 2005. Evidence for an association between heat shock protein 70 and the respiratory syncytial virus polymerase complex within lipid-raft membranes during virus infection. Virology 338, 69–80.

Buck, K.W., 1996. Comparison of the replication of positive-stranded RNA viruses of plants and animals. Adv. Virus Res. 47, 159–251.

Craig, E.A., Baxter, B.K., Becker, J., Halladay, J., Ziegelhoffer, T., 1994. Cytosolic hsp70s of *Saccharomyces cerevisae*: roles in protein synthesis, protein translocation, proteolysis and regulation. In: Morimoto, R.I., Tissieres, A., Georgopoulos, C. (Eds.), The biology of heat shock proteins and molecular chaperones. Cold Spring Harbor Laboratory Press, New York, pp. 31–52.

Daros, J.-A., Schaad, M.C., Carrington, J.C., 1999. Functional analysis of the interaction between VPg-proteinase (NIa) and RNA polymerase (NIb) of *Tobacco etch potyvirus*, using conditional and suppressor mutants. J. Virol. 73, 8732–8740.

El-Hage, N., Luo, G., 2003. Replication of hepatitis C virus RNA occurs in a membrane-bound replication complex containing nonstructural viral proteins and RNA. J. Gen. Virol. 84, 2761–2769.

Fauquet, C., Mayo, M., Maniloff, J., Desselberger, U., Ball, L.A., 2005. Virus Taxonomy: VIIIth Report of the International Committee on Taxonomy of Viruses. Elsevier Academic Press, San Diego.

Fellers, J., Wan, J., Hong, Y., Collins, G.B., Hunt, A.G., 1998. *In vitro* interactions between a potyvirus-encoded, genome-linked protein and RNA-dependent RNA polymerase. J. Gen. Virol. 79, 2043–2049.

Glotzer, J.B., Saltik, M., Chiocca, S., Michou, A.-I., Moseley, P., Cotten, M., 2000. Activation of heat-shock response by an adenovirus is essential for virus replication. Nature 407, 207–211.

Guo, D., Rajamaki, M.-L., Saarma, M., Valkonen, J.P.T., 2001. Towards a protein interaction map of potyviruses: protein interaction matrixes of two potyviruses based on the yeast two-hybrid system. J. Gen. Virol. 82, 935–939.

Herold, J., Andino, R., 2001. Poliovirus RNA replication requires genome circularization through a protein–protein bridge. Mol. Cell 7, 581–591.

Hofius, D., Maier, A.T., Dietrich, C., Jungkunz, I., Bornke, F., Maiss, E., Sonnewald, U., 2007. Capsid protein-mediated recruitment of host dnaJ-like proteins is required for *Potato virus Y* infection in tobacco plants. J. Virol. 81, 11870–11880.

Hong, Y., Hunt, A.G., 1996. RNA polymerase activity catalyzed by a potyvirus-encoded RNA-dependent RNA polymerase. Virology 226, 146–151.

Hong, Y., Levay, K., Murphy, J.F., Klein, P.G., Shaw, J.G., Hunt, A.G., 1995. A potyvirus polymerase interacts with the viral coat protein and VPg in yeast cells. Virology 214, 159–166.

Hu, J., Flores, D., Toft, D., Wang, X., Nguyen, D., 2004. Requirement of heat shock protein 90 for human hepatitis B virus reverse transcriptase function. J. Virol. 78, 13122–13131.

Hu, J., Toft, D., Anselmo, D., Wang, X., 2002. *In vitro* reconstitution of functional hepadnavirus reverse transcriptase with cellular chaperone proteins. J. Virol. 76, 269–279.

Jiang, Y., Serviene, E., Gal, J., Panavas, T., Nagy, P.D., 2006. Identification of essential host factors affecting Tombusvirus RNA replication based on the yeast Tet promoters Hughes collection. J. Virol. 80, 7394–7404.

Jones, A.L., Johansen, I.E., Bean, S.J., Bach, I., Maule, A.J., 1998. Specificity of resistance to pea seed-borne mosaic potyvirus in transgenic peas expressing the viral replicase (Nlb) gene. J. Gen. Virol. 79, 3129–3137.

Kampmueller, K.M., Miller, D.J., 2005. The cellular chaperone heat shock protein 90 facilitates flock house virus RNA replication in *Drosophila* cells. J. Virol. 79, 6827–6837.

Kushner, D.B., Lindenbach, B.D., Grdzelishvili, V.Z., Noueiry, A.O., Paul, S.M., Ahlquist, P., 2003. Systematic, genome-wide identification of host genes affecting replication of a positive-strand RNA virus. Proc. Natl. Acad. Sci. U. S. A. 100, 15764–15769.

Laemmli, U., 1970. Cleavage of structural proteins during the assembly of the head of bacteriophage T4. Nature 15, 680–685.

Léonard, S., Viel, C., Beauchemin, C., Daigneault, N., Fortin, M.G., Laliberté, J.-F., 2004. Interaction of VPg-Pro of *Turnip mosaic virus* with the translation initiation factor 4E and the poly(A)-binding protein *in planta*. J. Gen. Virol. 85, 1055–1063.

Li, X.H., Valdez, P., Olvera, R.E., Carrington, J.C., 1997. Functions of the *Tobacco etch virus* RNA polymerase (NIb): subcellular transport and protein–protein interaction with VPg/proteinase (NIa). J. Virol. 71, 1598–1607.

Lin, B., Wang, J., Liu, H., Chen, R., Meyer, Y., Barakat, A., Delseny, M., 2001. Genomic analysis of the Hsp70 superfamily in *Arabidopsis thaliana*. Cell Stress Chaperones 6, 201–208.

Mangus, D., Evans, M., Jacobson, A., 2003. Poly(A)-binding proteins: multifunctional scaffolds for the post-transcriptional control of gene expression. Genome Biol. 4, 1–14.

Martin, M.T., Cervera, M.T., Garcia, J.A., 1995. Properties of the active Plum pox potyvirus RNA polymerase complex in defined glycerol gradient fractions. Virus Res. 37, 127–137.

Martin, M.T., Garcia, J.A., 1991. Plum pox potyvirus RNA replication in a crude membrane fraction from infected *Nicotiana clevelandii* leaves. J. Gen. Virol. 72, 785–790.

Martinez-Trujillo, M., Limones-Briones, V., Cabrera-Ponce, J., Herrera-Estrella, L., 2004. Improving transformation efficiency of *Arabidopsis thaliana* by modifying the floral dip method. Plant Mol. Biol. Rep. 22, 63–70.

Mayer, M., Bukau, B., 2005. Hsp70 chaperones: cellular functions and molecular mechanism. Cell. Mol. Life Sci. 62, 670–684.

Mayer, M.P., 2005. Recruitment of Hsp70 chaperones: a crucial part of viral survival strategies. Rev. Physiol., Biochem. Pharmacol. 153, 1–46.

Momose, F., Naito, T., Yano, K., Sugimoto, S., Morikawa, Y., Nagata, K., 2002. Identification of Hsp90 as a stimulatory host factor involved in influenza virus RNA synthesis. J. Biol. Chem. 277, 45306–45314.

Nicolas, O., Laliberté, J.F., 1992. The complete nucleotide sequence of *Turnip mosaic potyvirus* RNA. J. Gen. Virol. 73, 2785–2793.

Nishikiori, M., Dohi, K., Mori, M., Meshi, T., Naito, S., Ishikawa, M., 2006. Membrane-bound *Tomato mosaic virus* replication proteins participate in RNA synthesis and are associated with host proteins in a pattern distinct from those that are not membrane bound. J. Virol. 80, 8459–8468.

Osman, T.A., Buck, K.W., 1997. The *Tobacco mosaic virus* RNA polymerase complex contains a plant protein related to the RNA-binding subunit of yeast eIF-3. J. Virol. 71, 6075–6082.

Panavas, T., Serviene, E., Brasher, J., Nagy, P.D., 2005. Yeast genome-wide screen reveals dissimilar sets of host genes affecting replication of RNA viruses. Proc. Natl. Acad. Sci. U. S. A. 102, 7326–7331.

Prokhnevsky, A.I., Peremyslov, V.V., Dolja, V.V., 2005. Actin cytoskeleton is involved in targeting of a viral Hsp70 homolog to the cell periphery. J. Virol. 79, 14421–14428.

Quadt, R., Kao, C.C., Browning, K.S., Hershberger, R.P., Ahlquist, P., 1993. Characterization of a host protein associated with *Brome Mosaic Virus* RNA-dependent RNA polymerase. Proc. Natl. Acad. Sci. U. S. A. 90, 1498–1502.

Restrepo-Hartwig, M.A., Carrington, J.C., 1994. The *Tobacco etch potyvirus* 6-kilodalton protein is membrane associated and involved in viral replication. J. Virol. 68, 2388–2397.

Restrepo, M.A., Freed, D.D., Carrington, J.C., 1990. Nuclear transport of plant potyviral proteins. Plant Cell 2, 987–998.

Riedel, D., Lesemann, D.E., Maiß, E., 1998. Ultrastructural localization of nonstructural and coat proteins of 19 potyviruses using antisera to bacterially expressed proteins of plum pox potyvirus. Arch. Virol. 143, 2133–2158.

Rigaut, G., Shevchenko, A., Rutz, B., Wilm, M., Mann, M., Séraphin, B., 1999. A generic protein purification method for protein complex characterization and proteome exploration. Nat. Biotechnol. 17, 1030–1032.

Rohila, J.S., Chen, M., Cerny, R., Fromm, M.E., 2004. Improved tandem affinity purification tag and methods for isolation of protein heterocomplexes from plants. Plant J. 38, 172–181.

Rubio, V., Shen, Y., Saijo, Y., Liu, Y., Gusmaroli, G., Dinesh-Kumar, S.P., Deng, X.W., 2005. An alternative tandem affinity purification strategy applied to *Arabidopsis* protein complex isolation. Plant J. 41, 767–778.

Sanchez, F., Martinez-Herrera, D., Aguilar, I., Ponz, F., 1998. Infectivity of *Turnip mosaic potyvirus* cDNA clones and transcripts on the systemic host *Arabidopsis thaliana* and local lesion hosts. Virus Res. 55, 207–219.

Schaad, M., Jensen, P., Carrington, J., 1997. Formation of plant RNA virus replication complexes on membranes: role of an endoplasmic reticulum-targeted viral protein. EMBO J. 16, 4049–4059.

Schwartz, M., Chen, J., Janda, M., Sullivan, M., den Boon, J., Ahlquist, P., 2002. A positive-strand RNA virus replication complex parallels form and function of retrovirus capsids. Mol. Cell 9, 505–514.

Serva, S., Nagy, P.D., 2006. Proteomics analysis of the Tombusvirus replicase: Hsp70 molecular chaperone is associated with the replicase and enhances viral RNA replication. J. Virol. 80, 2162–2169.

Simon-Mateo, C., Lopez-Moya, J.J., Guo, H.S., Gonzalez, E., Garcia, J.A., 2003. Suppressor activity of potyviral and cucumoviral infections in potyvirus-induced transgene silencing. J. Gen. Virol. 84, 2877–2883.

Stahl, M., Retzlaff, M., Nassal, M., Beck, J., 2007. Chaperone activation of the hepadnaviral reverse transcriptase for template RNA binding is established by the Hsp70 and stimulated by the Hsp90 system. Nucleic Acids Res. 35, 6124–6136.

Sullivan, C.S., Pipas, J.M., 2001. The virus–chaperone connection. Virology 287, 1–8.

Sung, D.Y., Vierling, E., Guy, C.L., 2001. Comprehensive expression profile analysis of the *Arabidopsis* Hsp70 gene family. Plant Physiol. 126, 789–800.

Tomita, Y., Mizuno, T., Diez, J., Naito, S., Ahlquist, P., Ishikawa, M., 2003. Mutation of host dnaJ homolog inhibits *Brome mosaic virus* negative-strand RNA synthesis. J. Virol. 77, 2990–2997.

Wang, X., Ullah, Z., Grumet, R., 2000. Interaction between *Zucchini yellow mosaic potyvirus* RNA-dependent RNA polymerase and host poly(A)-binding protein. Virology 275, 433–443.

Yamada, K., Lim, J., Dale, J.M., Chen, H., Shinn, P., Palm, C.J., Southwick, A.M., Wu, H.C., Kim, C., Nguyen, M., Pham, P., Cheuk, R., Karlin-Newmann, G., Liu, S.X., Lam, B., Sakano, H., Wu, T., Yu, G., Miranda, M., Quach, H.L., Tripp, M., Chang, C.H., Lee, J.M., Toriumi, M., Chan, M.M.H., Tang, C.C., Onodera, C.S., Deng, J.M., Akiyama, K., Ansari, Y., Arakawa, T., Banh, J., Banno, F., Bowser, L., Brooks, S., Carninci, P., Chao, Q., Choy, N., Enju, A., Goldsmith, A.D., Gurjal, M., Hansen, N.F., Hayashizaki, Y., Johnson-Hopson, C., Hsuan, V.W., Iida, K., Karnes, M., Khan, S., Koesema, E., Ishida, J., Jiang, P.X., Jones, T., Kawai, J., Kamiya, A., Meyers, C., Nakajima, M., Narusaka, M., Seki, M., Sakurai, T., Satou, M., Tamse, R., Vaysberg, M., Wallender, E.K., Wong, C., Yamamura, Y., Yuan, S., Shinozaki, K., Davis, R.W., Theologis, A., Ecker, J.R., 2003. Empirical analysis of transcriptional activity in the *Arabidopsis* genome. Science 302, 842–846.

Yamaji, Y., Kobayashi, T., Hamada, K., Sakurai, K., Yoshii, A., Suzuki, M., Namba, S., Hibi, T., 2006. *In vivo* interaction between *Tobacco mosaic virus* RNA-dependent RNA polymerase and host translation elongation factor 1A. Virology 347, 100–108.

Zhang, S.C., Zhang, G., Yang, L., Chisholm, J., Sanfacon, H., 2005. Evidence that insertion of *Tomato ringspot nepovirus* NTB-VPg protein in endoplasmic reticulum membranes is directed by two domains: a C-terminal transmembrane helix and an N-terminal amphipathic helix. J. Virol. 79, 11752–11765.

Zylicz, M., Ang, D., Liberek, K., Georgopoulos, C., 1989. Initiation of lambda DNA replication with purified host- and bacteriophage-encoded proteins: the role of the dnaK, dnaJ and grpE heat shock proteins. EMBO J. 8, 1601–1608.